Sensing and Bio-Sensing Research 32 (2021) 100425

Contents lists available at ScienceDirect

Sensing and Bio-Sensing Research

journal homepage: www.elsevier.com/locate/sbsr

Green synthesis of silver nanoparticle using *goniothalamus wightii* on graphene oxide nanocomposite for effective voltammetric determination of metronidazole

Santhosh Chinnaraj [a], Vino Palani [a], Sudesh Yadav [b], Maruthupandian Arumugam [a,*], Mani Sivakumar [c,*], Viji Maluventhen [d], Mandeep Singh [e]

[a] Ethnopharmacology and Algal Biotechnology Division, Department of Botany, Periyar University, Salem, Tamilnadu 636 011, India
[b] Centre for Green Technology, School of Civil and Environmental Engineering, University of Technology Sydney, 15 Broadway, NSW 2007, Australia
[c] Advanced Membrane Materials Research Center, Graduate Institute of Applied Science and Technology, National Taiwan University of Science and Technology, No. 43, Section 4, Keelung Rd, Da'an District, Taipei City 10607, Taiwan
[d] Department of Botany, Thiagarajar College, Madurai, Tamilnadu 625009, India
[e] School of Mechanical and Mechatronic Engineering, University of Technology Sydney, 15 Broadway, NSW 2007, Australia

ARTICLE INFO

Keywords:
Green synthesis
AgNPs
GO@AgNPs composite
Metronidazole
electrochemical sensor

ABSTRACT

Graphene oxide (GO) has piqued the interest of both academia and industry owing to its polar and two-dimensional (2D) layered structure. Antibiotic concentrations can be detected with advanced GO composites to reduce the risk of bacterial resistance, which can be done with electrochemical sensors. Herein, we have developed an eco-friendly synthesis approach, one-pot strategy towards *Goniothalamus wightii* biomass-derived solution preparation of Ag nanoparticle-decorated graphene oxide (GO@AgNPs) composites. As- synthesized GO@AgNPs nanocomposites were analyzed using various analytical tools including Raman, X-ray diffraction (XRD) and field emission scanning electron microscope (FESEM). The Metronidazole (MIZ) determination was then investigated using cycle volumetric and amperometric (*i-t*) techniques by the GO@AgNPs composites. Prepared composites exhibit a wide-linear range of 0.09 μM to 4.594 mM, low detection limit of 69 nM and a limit of quantification detection of 786 nM. Furthermore, the practical applicability of the prepared GO@AgNPs nanocomposites were examined in pharmaceutical drug Flagyl (500 mg) with satisfactory recovery results.

1. Introduction

In modern materials science, the field of nanotechnology is one of the most prominent fields of study. Nanoparticles have enhanced properties based on special features, including size, distribution, and morphology [1]. Nanoparticles can be categorized by size, morphology, and physicochemical properties into various groups. They include carbon nanoparticles, ceramic nanoparticles, metal nanoparticles, polymer nanoparticles, and lipid-based nanoparticles. Nanotechnology includes the use of materials with components with dimensions of less than 100 nm [2]. Nanotechnology provides sustainable agricultural potential solutions, including improving efficiencies in nutrient usage, enhancing the effectiveness of pest control, mitigating the impacts of climate change, and reducing the negative environmental consequences of agricultural food production [3]. Several innovative nanotechnologies were being developed and implemented at different scales, but the introduction of technology must overcome many barriers to implementation, including efficient distribution at the field scale, regulatory and safety issues, and customer acceptance [4].

The use of science to control matter at the molecular level is emerging rapidly, such as nanotechnology, bio-nanotechnology. A wide range of silver nanoparticles is developed by a variety of methods [5]. Ecologically friendly procedures for the prevention of toxic chemicals in the synthesis frameworks need to be formulated to avoid adverse effects in medical applications. A daily increase in demand for green nanoparticle synthesis is caused by chemical synthesis disadvantages. The numerous phytochemicals in medicinal plant extracts are used to reduce and stabilize nanoparticles such as flavonoids, alkaloids, terpenoids,

* Corresponding authors.
E-mail addresses: maruthumdu82@gmail.com, maruthubot@periyaruniversity.ac.in (M. Arumugam), sivakumar@mail.ntust.edu.tw, sivaphy05@gmail.com (M. Sivakumar).

https://doi.org/10.1016/j.sbsr.2021.100425
Received 17 February 2021; Received in revised form 21 April 2021; Accepted 26 April 2021
Available online 28 April 2021

amides, and aldehydes [6]. Nanoparticles green syntheses, in particular Fe, Pd, Ag, Au, Cu, CdS, CuO, Ru, PbS, Fe_3O_4, ZnO, TiO_2, and CeO_2, use biological components of medicinal plants that examine the function of different applications [7]. Traditional medicines are widely used in Southeast Asian countries due to their low toxicity, low cost, and ease of use when compared to synthetic drugs. Many bioactive compounds are found in medicinal plant-derived products, which improves therapeutic value and novel drug development [8]. About 160 species of the *Annonaceae* family belong to the *Goniothalamus* genera, which are found in tropical and subtropical regions [9]. *Goniothalamus wightii* Hook. F. & Thomas (Local name: pulithali, kattunarai pachallai, locally recognised plants) is a small pungent-odor tree whose leaves and fruits have a naturally bitter flavour and are normally consumed in a paste form and taken orally for relief from rheumatic pain and other medicinal applications [9]. Bio compounds of alkaloids, glycosides, tannins, saponins, and aromatic compounds have been identified in this species and are used in a variety of biological applications as well as for green nanoparticle synthesis [10].

Resistance to silver nanoparticles (Ag NPs) has now become less likely to bacteria than traditional antibiotics [11]. Graphene oxide (GO) is recently also the possible substance that is commonly used, one of which is antibacterial therapy [12]. The antimicrobial concept can be extracted from GO bacteria traps when Ag destroys bacteria. Thus the combination of GO and Ag NPs may indicate that biocompatibility, easy synthesis, and low cost make them efficient [13].

GO has the hydrophilic character of making it water-soluble nanomaterial because of the presence of polar functional groups such as carbonyl, epoxy, and carboxylic acid [14]. Besides, GO's surface functionality has provided many opportunities for its use in the production of nanocomposite materials [15,16]. GO is highly conductive and has numerous applications in the area such as anti-cancer, electronics, antibacterial biomedicine coatings, photocatalytic action, water decontamination, solar desalination, drug provision, and most importantly sensors [16]. The nanocomposite, however, strengthens GO properties [17,18]. Silver (Ag) is the most reactive and conductive material of all transitional elements and has been used in the recent development of Ag-doped GO with low resistance, stable dispersion, and improved mechanical strength characteristics [17,19]. AgNPs have recently received considerable attention in antibacterial applications due to their bactericidal nature [20]. AgNPs are spread on the surface of GOs and interspersed among the layers of GO to research the electrochemical properties and the photocatalytic sample degradation rate [19].

Metronidazole, one of the best-known nitroimidazole derivatives, is selective against trichomonas [21]. But metronidazole overuse and long-term use can cause toxicity, peripheral neuropathy, and optic neuropathy [22]. Therefore, metronidazole concentration in antibiotic therapy patients must be controlled. Several analytical methods for metronidazole determination, including spectrophotometry and chromatography, have been published [23,24]. However, these approaches could not achieve high metronidazole selectivity, which was expensive and time-consuming. An alternative method for the determination of metronidazole with high sensitivity and selectivity is, therefore, necessary to establish [25]. Electrochemical sensor determination provides the advantages of low cost, high sensitivity, and fast operation, generally applied in analytical chemistry, and separation steps are normally used to improve selectivity before identification [18].

In this work, we targeted AgNPs using *Goniothalamus wightii* leaves and interrelated them with GO nanocomposites to effectively detect metronidazole. Physicochemical properties were investigated using various techniques such as field emission morphology scanning electron microscopy (FESEM), X-ray difference (XRD), Raman spectroscopy. Also, AgNPs@GO composite modified electrode was used cycle voltammetry (CV), and amperometric (*i-t*) to electrochemically evaluate MTZ. Then the MTZ's piratical determination was suggested after the modified electrode AgNPs@GO nanocomposites.

2. Materials and methods

2.1. Materials

Silver nitrate ($AgNO_3$; ≥99.0%), glucose ($C_6H_{12}O_6$; ≥99.5%), lactose ($C_{12}H_{22}O_{11}{\cdot}H_2O$; ≥99%), sucrose ($C_{28}H_{38}O_{19}$; ≥99.5%), potassium chloride (KCl; 100%), lithium chloride (LiCl; ≥99.0%), sodium chloride (NaCl; ≥99.0%), monosodium (NaH_2PO_4; ≥99.0%), disodium (Na_2HPO_4; ≥99.0%), 4-nitroaniline (4NA; ≥99.0%), and Nickel (II) chloride ($NiCl_2.6H_2O$; 98%) were obtained from Sigma-Aldrich. nilutamide (NIL; ≥98.0%), 4-nitrobenzene (4NB; ≥97.0%), flutamide (FLA; ≥99.0%), 4-nitrophenol (4NP; ≥99.0%) were bought from Alfa Aesar. All chemicals were used a without any cleansing. The glassy carbon electrode (GCE) was obtained from Sigma Aldrich. The rotating ring disk electrode of glassy carbon electrode was bought from Pine Research Instrumentation, Inc., Durham, NC 27705 USA (Pine AFMSRX Electrode Rotator). For the preparation of the working electrolyte phosphate buffer (0.05 M PB, pH = 7.2) and monosodium (NaH_2PO_4) and disodium (Na_2HPO_4) were used. For the preparation of various PB (pH = 3, 5, 7, 9, and 11), HCl/NaOH was used.

2.2. Collection of sample and identification

Freshly young leaves of *Goniothalamus wightii* were collected in July 2019 in Kalakad Mundanthurai Tiger Reserve Forest, Tirunelveli district Tamilnadu, India with help of local Kanikkars tribals. The plant was identification and authentication in the department of Botany, Periyar University, Salem, Tamilnadu, India. A voucher specimen with reference number (PU/BOT/HVO.177) was afterward the submitted herbarium of the University.

2.2.1. Synthesis of silver nanoparticles

Goniothalamus wightii extract preparation: The samples were thoroughly washed with distilled water, diced into small parts, and then dried in the shade. The dried Goniothalamus wightii leaves (25 g) were finely ground and powdered. For 24 h, 2 g of biomass (G wightii leaves) was kept in a 250 mL conical flask with 100 mL of distilled water. Finally, the extract was filtered with Whatman no. 1 filter paper and stored at 4 °C for further analysis [26].

A simple approach of AgNPs synthesis method: For the synthesis of silver nanoparticles, aqueous solution (1 mM) of silver nitrate ($AgNO_3$) was usually prepared using a standard process. For reduction into Ag^+ ions, 10 mL of G wightii leaf extract was added into 90 mL of aqueous solution (1 mM; silver nitrate). The colour of silver nitrate reduced to silver changed from colourless to brown (Scheme 1). The centrifuge was rotating at 5000 rpm for 30 min. The top layer was separated from the bottom layer, which was redissolved in deionized water. The particle was centrifuged several times to remove any contaminants that had been absorbed on the surface of the silver nanoparticles.

2.3. Synthesis of GO@AgNPs

Firstly, GO was synthesized *via* modified Hummer's method [17] using graphite powder, $NaNO_3$, H_2SO_4, and H_2O_2 (30%) as the starting materials. To disperse the GO material into individual sheets, GO was dissolved in a solution of distilled water and sonicated. To prepare GO-AgNPs nanocomposite, firstly GO sheets were exfoliated by adding 1 mg/mL of GO in 10 mL of DI in an ultrasonic bath for 1 h. Then 10 ml of 0.05 mg/ml AgNPs solution was slowly dropwise added to the GO suspension was stirred for 60 min to allow Ag^+ ions to interact with the GO sheets. Finally, the GO@AgNPs nanocomposite was separated into the different subunits at −140 °C, and held for 12 h.

2.4. Characterization of GO@AgNPs composites

The current surface morphology was explored through micro-scopic

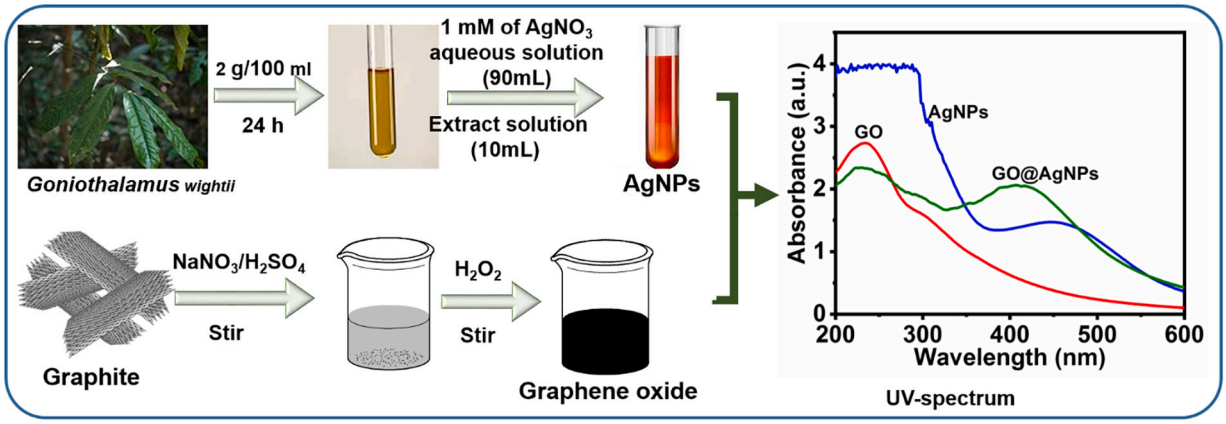

Scheme 1. Synthesis procuress of Ag nanoparticles by *G wightii* extract solution, graphite derived graphene oxide, and Ag nanoparticle-decorated graphene oxide (GO@AgNPs) composites for UV-spectrum.

analysis with scanning electron microscopy. UV–Vis absorption spectrum was analyzed using Thermo Scientific Multiscan Spectrum 1500, USA. X-ray diffraction was examined by Bruker, D2 Phaser X-ray Diffraction on a desktop (Cu Kα λ = 0.154060 nm). Raman spectrum analysis was conducted with Micro Raman Spectra (using the 532 nm excitation laser). Electrochemical impedance spectroscopy (EIS) was used to the IM6ex ZAHNER impedance measurement unit with a frequency range of 100 mHz to 100 kHz. CV and (*i-t*) studies were performed using the CHI 620a electrochemical work station. Studies involving electrochemical analysis of three different three-electrode systems were conducted using Ag/AgCl (saturated KCl) as the working electrode, and platinum wire as the counter-electrode. All the electrochemical measurements were taken with the equipment cold.

2.5. The preparation of GO@AgNPs composites modified electrode

Typically, 6 mg/mL of GO@AgNPs composites was dispersed in DI solution at an ultra-sonication for 15 min. And 6 μL of the well-dispersed solution was drop casted on a clean glassy carbon electrode (GCE) surface at dried 30 °C. All electrochemical tests were conducted in the same manner on a varied electrode.

3. Results and discussion

3.1. Characterization of synthesis materials

Scheme 1 shown the AgNPs absorption spectrum of UV–spectrum, and its present a broad bell-shaped spectrum curve. The plant extract introduced to solution make a uarious metabolites from the spectrophotometric range at 445 nm. The AgNPs was synthesized using an eco-friendly approach, and it can be the spherical in nature of particle size. Besides, the GO was synthesized using graphite powder through a modified Hummer's method [17], and the UV spectrum peaks at 233 and 302 nm are attributable to C—C and C═O interactions of graphene oxide layers for (π—π *). The marginally shifted AgNPs peak at 415 nm and GO peak at 231 and 296 nm is observed in the GO@AgNPs composite due to well-interaction.

The surface morphology of AgNPs, GO, and GO@AGNPs composites

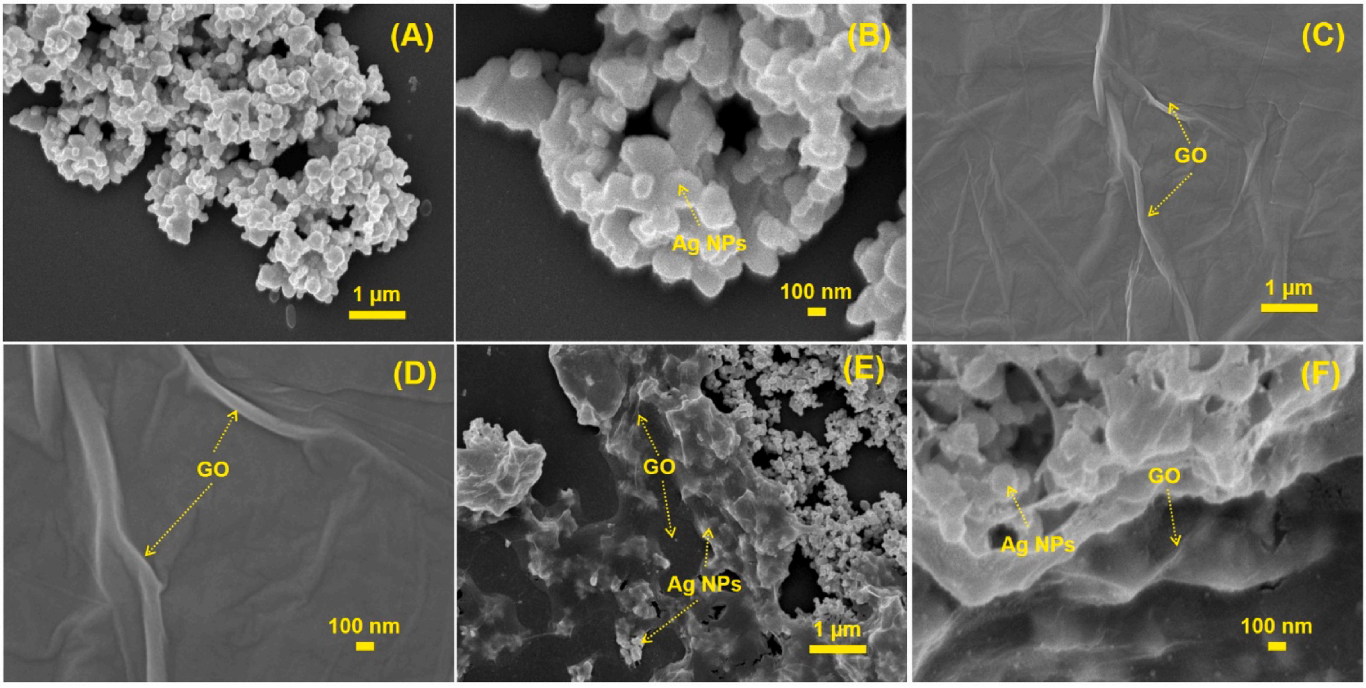

Fig. 1. SEM images of AgNPs@GO nanocomposites at different magnification.

is shown in Fig. 1. As-synthesis of Ag NPs shown the clear nanoparticle morphology in Fig. 1(A,B). The graphene oxide nano-layers sheet was observed in Fig. 1(C,D). Then the GO interacted with Ag NPs composites shown in the clear image in Fig. 1(E,F). We can confirm the Ag^{+} ions intercalated with a GO nanosheet surface. Then the ImageJ software was used to analyse the average particle size of AgNPs, which was around 174.26 nm as shown in Fig. S1.

XRD spectrum and Raman spectrum were analyzed the nanoparticle composites formation. Fig. 2A, the crystallite of Ag NPs has confirmed the 2θ values of 28.13°, 32.5°, 38.34°, 46.44°, 54.98°, and 57.69°, due to the (110), (122), (123), (231), (142) and (241) lattice planes to corresponding the space group of a faced center cubic (FCC) for Ag nanoparticle, respectively. That the Ag nanoparticles are confirmed the crystalline nature (JCPDS File No. 84–0713) [23] and the Ag NPs has shown the high purity nature intercalated with GO composites for enhancing electro-catalytic properties.

Fig. 2B, the GO exhibit the D and G band peaks of 1353.53 and 1593.57 cm^{-1} to confirm the D band defecting of the oxidation group, and I_D/I_G ratio value was 0.76. [13] the Ag NPs exhibits 458.69, 619.92, 964.66, 1069.36, 1113.86, and 1204.33 cm^{-1} due to the formation of nanoparticle confirmation at the high peak intensity of 964.66 cm^{-1}. Then the Ag NPs intercalated with GO nanolayers shown the D and G band ratio of 0.77 due to the slight increase to confirm the composites.

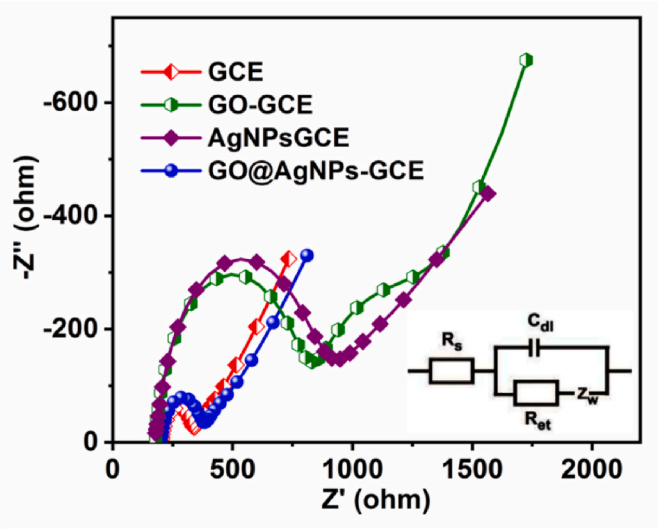

Fig. 3. EIS studies of modified electrode and without modified electrode in 5 mM of $[Fe(CN)_6]^{-3/-4}$ containing 0.1 M KCl solution at applied frequency range of 100 mHz to 100 kHz and voltage of 5 V.

3.2. Electrochemical performance of the modified electrodes

3.2.1. Electrochemical impedance spectroscopy studies

The electrochemical impedance spectroscopy (EIS) studies shows the electron transfer rate related to resistance value in5 mM of $[Fe(CN)_6]^{-3/-4}$ containing 0.1 M KCl solution at the frequency range of 100 mHz to 100 kHz and applied voltage of 5 V as shown in Fig. 3. The circuit model of Randles shown the Fig. 3(Inset), Charge transmission resistance, electrolyte resistance, Warburg impedance, and double layer capacitance were represented by R_{ct}, R_s, Z_w, and C_{dl}, respectively. The EIS plot shows that both the modified and bare electrode had semicircles of varying diameters, which corresponded to various R_{ct} values. The R_{ct} values were 653.87 Ω, 754.69 Ω, 179.28 Ω, and 137.06 Ω from GO-GCE, AgNPs-GCE, GO@AgNPs-GCE, and bare GCE, respectively. Furthermore, GO@AgNPs-GCE exhibits the low resistance *vs* high electron transfer to determination of MIZ.

3.2.2. Electrochemical behavior of different modified electrodes at MIZ

Fig. 4A depicts the CV profiles in the absence (d) and presence of metronidazole (MIZ - 385 μM) at different modified electrodes ((a') bare GCE, (b') AgNPs-GCE, (c') GO-GCE, and (d') AgNPs@GO-GCE recorded in 0.05 M PB at 50 mV s^{-1} of sweep rate. From Fig. 4A(a') in presence of MIZ, the bare GCE delivers poor cathodic current (16.74 μA) with greater potential (−0.84 V). When bare GCE was modified with AgNPs

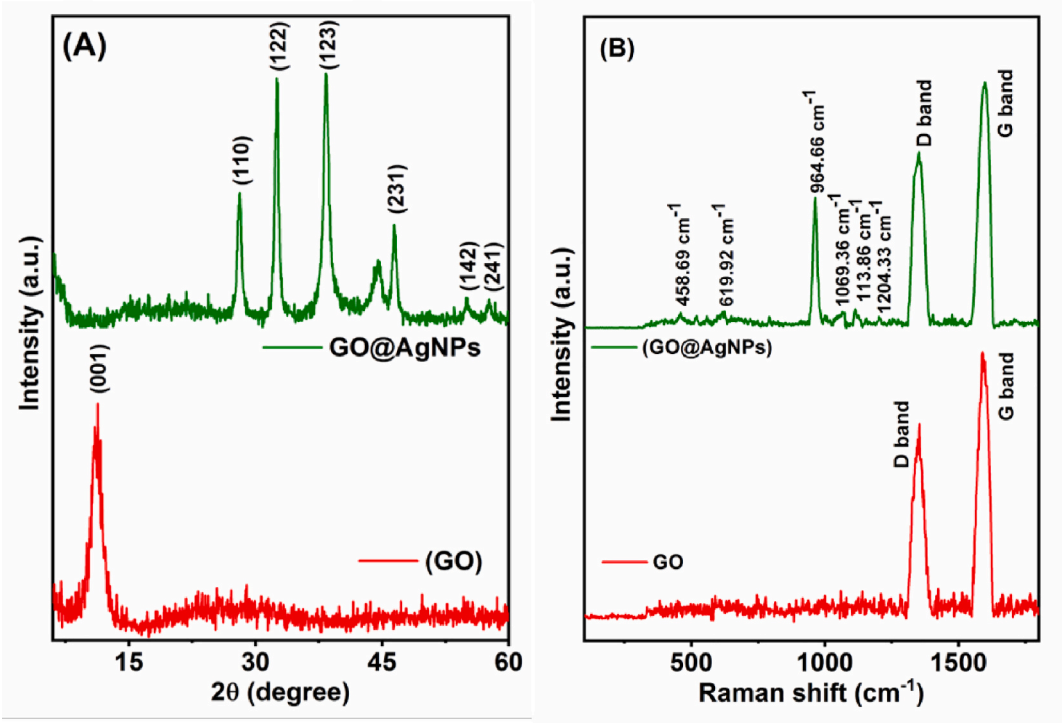

Fig. 2. (A) XRD pattern of GO and GO@AgNPs composites. (B) Raman spectrum of GO and GO@AgNPs composites.

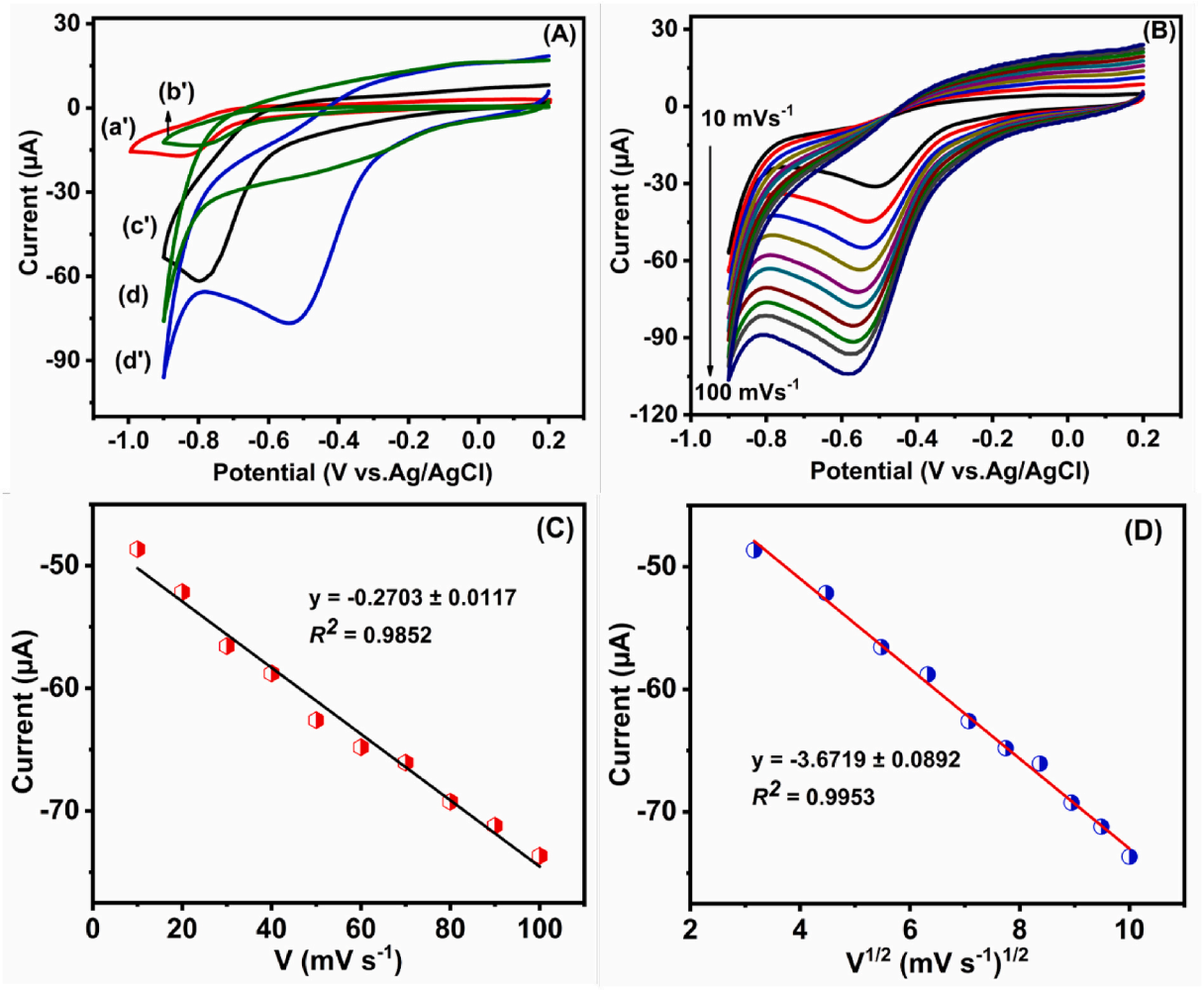

Fig. 4. (A) CV curves of (a') bare GCE, (b') AgNPs-GCE, (c') GO-GCE, (d') AgNPs@GO-GCE, and (d) AgNPs@GO-GCE recorded in the presence and absence of MIZ (385 μM) in 0.05 M PBS (pH 7.2) at a scan rate of 50 mV s^{-1}. (B) CV profiles obtained at different scan rates: 10 to 100 mV s^{-1} to corresponding the plot of reduction peak current *vs.* scan rate (C) and log(scan rate) *vs.* reduction peak current (D).

Fig. 4A(b') the cathodic peak (13.17 μA) potential proceeds with a positive shift (−0.78 V) compared to bare GCE signifies the involvement of AgNPs towards the detection of MIZ. The enhancement in the cathodic current was found on modifying bare GCE with GO Fig. 4A(c') this was due to the stacking arrangement of graphene oxide layers over the surface of GCE induces the electron transfer pathway between the electrode interface. The maximum current (76.88 V) was attained with lower cathodic potential (−0.54 V) on AgNPs@GO composite modified electrode because of interaction between the AgNPs and π- π stacking arrangement of GO. The unification of AgNPs in carbon lattice further enhances the electron transfer kinetics. Hence AgNPs@GO composite is considered to be an efficient electrode modifier with low potential detection of MIZ compared to other modified electrodes.

3.2.3. *Effect of sweep rate of MIZ on AgNPs@GO-GCE*

Fig. 4B signifies the CVs for various sweep rates (10–100 mV s^{-1}) in presence of 385 μM MIZ in 0.05 M PB. The cathodic current elevated linearly while increasing the sweep rate from 10 to 100 mV s^{-1} with a trivial shift in the cathodic current potential indicates the electrocatalytic activity of AgNPs@GO-GCE sweep rate dependent. Further, the linear dependence plot scan rate *vs* peak current and square root of sweep rate *vs* current were shown in Fig. 4(C,D), and the correlation coefficient (R^2 = 0.9851 and 0.9953) expresses the diffusion control reaction was followed in the detection of MIZ at AgNPs@GO-GCE rather than diffusion-controlled process.

3.2.4. *Effect of pH, and concentration of MIZ at AgNPs@GO-GCE*

The impact of pH determines the peak shape, cathodic current, cathodic potential, *etc.* Hence, the CV was performed with varying pH (3, 5, 7, 9, and 11). The CV platform of different operation potential in Fig. 5A portraits noticeable current changes. While increasing the pH from pH = 3 to 7 the cathodic current increases with a positive shift. Further, an increase of pH from pH 7 = 11 results in a negative shift along with a decrement in the cathodic current. The decrease and increase of cathodic current were displayed in Fig. 5B is a plot diagram.

And the linear calibration plot for pH *vs.* cathodic potential contains a correlation coefficient (R^2 = 0.995), indicating that an equal number of electrons and protons are involved in the electrochemical reaction, with the conversion of the nitro group to nitroso derivation followed by the conversion of the hydroxyl group. As a result of these findings, pH, 7 is revealed to be a more suitable electrolyte for the electrochemical behavior of MIZ at AgNPs@GO-GCE. Further, the higher electrocatalytic activity of MIZ at AgNPs@GO-GCE was scrutinized by altering the quantity of MIZ from 99 to 990 μM at 50 mV s^{-1} in 0.05 M PB. Fig. 5C shows linear increases of cathodic current while altering the quantity of MIZ expresses the higher electrocatalytic activity. Besides, Fig. 5D displays a calibration plot between the quantity of MIZ (μM) and cathodic current (I_{pc}) composed with the correlation coefficient (R^2 = 0.9973). Upon analyzing the effect on sweep rate, pH, and concentration of MIZ, AgNPs@GO composite is considered to be a prominent electrode modifier electrochemical detection MIZ sensor.

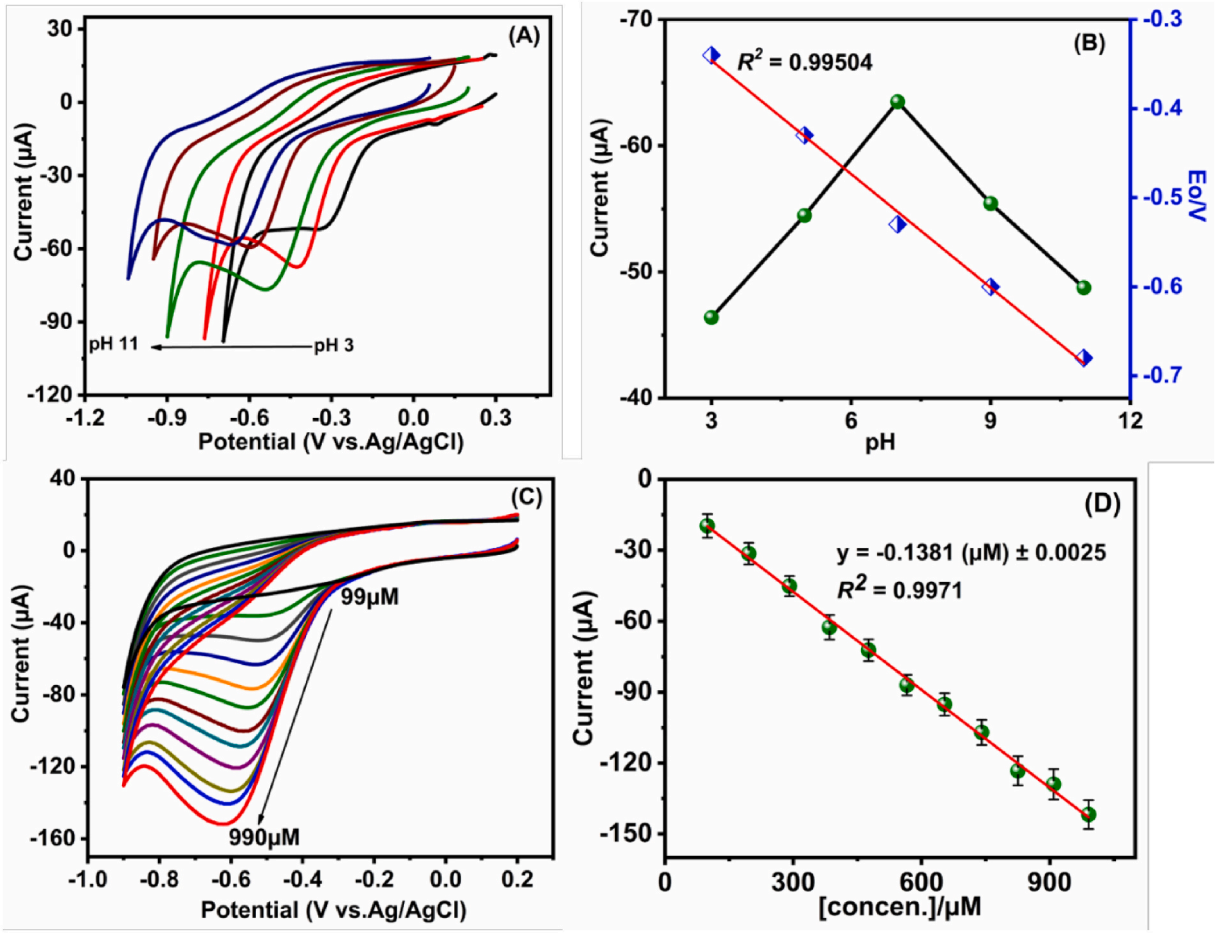

Fig. 5. (A) CV curves obtained different pH (3 to 11) with the presents of metronidazole (385 μM). (B) plot of peak current (E_p) *vs.* pH and plot of reduction peak current *vs.* pH. (C) CV curves of AgNPs@GO-GCE were obtained in the presence of different concentrations of metronidazole (385 μM) in 0.05 M PBS (pH 7.2) at a scan rate of 50 mV s^{-1} and (D) plot of reduction peak current *vs.* different concentration of metronidazole.

3.2.5. *Amperometric performance of MIZ at AgNPs@GO-GCE*

To determine the selectivity and sensitivity nature of the AgNPs@GO composite, amperometric (*I-t*) was preferred with AgNPs@GO-GCE as a rotating disc electrode. The experiment was carried out in 0.05 M PBS (pH 7.2) with a variable amount of MIZ (0.09 to 4594 M) at −0. 54 V with a rotating speed of 1500 rpm while the addition of MIZ.As, a result of the sequential addition of MIZ, the cathodic current was increased as observed in Fig. 6A. Fig. 6A(inset) demonstrates the *I-t* current found in the short period along with the lowest quantity of MIZ. Moreover, the linear calibration plot was plotted between the quantity of MIZ (μA) and current (μA) displayed in Fig. 6B exposed with linear regression (I_{pc} = −25.148 [mM of MIZ] – 0.2764) equation and calibration equation R^2 = 0.9974. The found slope of the linear regression equation was substituted in the limit of detection and sensitivity formulation (LOD = 3σ/S and LQD: 10*σ/S; S and σ denote slope of the calibration curve and standard deviation of blank; S is a sensitivity = slope value/working electrode surface area (0.196 cm^2)). The LOD and sensitivity were calculated to be 0.069 μM, 0.786 μM and 347.14 A mM^{-1} cm^2 after substituting. The attained analytical parameters (LOD, sensitivity, linear range) were compared with previously reported literature subjected in Table 1. From the literature survey, GO@AgNPs-GCE outcomes with excellent linear range, LOD, and sensitivity towards detection of MIZ.

The selectivity capability of GO@AgNPs-GCE was further examined with the same parameters of Fig. 6C. The sequential addition of varied electroactive compounds nilutamide (NIL), 4-nitrobenzene (4NB), flutamide (FLA), 4-nitroaniline (4NA), 4-nitrophenol (4NP), KCl, Li^+, NaCl, Ni, NO_2, SO_4^{2-}, glucose, lactose, and sucrose in presence of 100 μM of MIZ doesn't provide any amperometric signal suggesting excellent selectivity and potential towards the detection of MIZ sensor. Furthermore, GO@AgNPs-GCE exhibits long-term stability in MIZ presense at an applied potential range of −0.54 V for rpms ranging from 1200 to 2000 s in Fig. 6D. We have observed the retaining performance parentage of 94.8%, and it's suitable for further application.

3.2.6. *Investigation of the real sample at AgNPs@GO modified electrode*

The real sample analysis was performed on the pharmaceutical drug Flagyl (500 mg) obtained from a nearby pharmacy in Taipei, Taiwan, to evaluate the real-time applicability of the proposed sensor. The pharmaceutical drugs were then prepared as a real sample by ultrasonicating 10 mg of 10 mL DI water dispersion for 60 min, and the resulting solution was centrifuged at 5000 rpm for 15 min. Furthermore, the drug resultant solution was combined with a lab sample of each sample mixed in a 1:1 solution ratio. At each 50-s interval addition of 50 μL to 150 μL, the real sample of tablet, tablet mixed lab sample, and MIZ solution were added to 0.05 M PBS (pH 7.2) at applied potential −0.54 V; rpm: 1200. The experiment was achieved with the same parameters as Fig. 7. We have achieved the effect response of drug, mixed, and MIZ solution, and it can be suitable for further real-time applications.

4. Conclusion

We investigated AgNPs@GO nanocomposites, which are prepared *via* the green synthesis route. Herein, *Goniothalamus wightii* was used for the preparation of Ag nanoparticle and mixed with GO to obtain

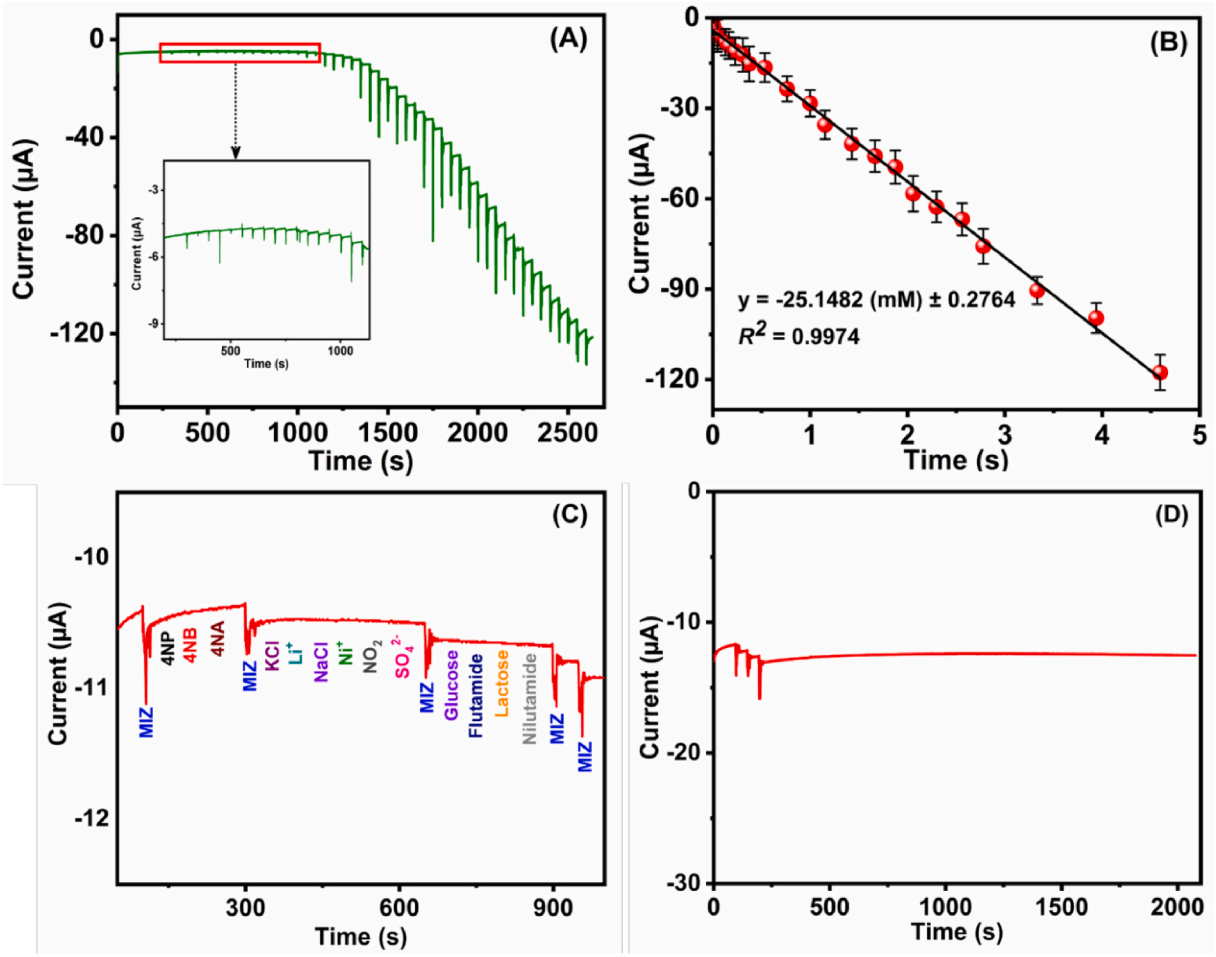

Fig. 6. (A) Amperometry response of AgNPs@GO-GCE in 0.05 M PBS (pH 7.2) at containing different concentrations of metronidazole (0.09 to 4594 μM), and (B) the plot of reduction peak current (*Ipa*) *vs* different concentration of metronidazole. (C) Amperometry response of various interference compound studies. (D) Amperometry profile of the stability studies in the presence of MIZ. [Applied potential: −0.54 V; rpm: 1200].

Table 1
Comparison of GO@AgNPs-GCE based MIZ sensor with reported MIZ sensors.

Modified electrode	Methods	LOD (μM)	Linear range (μM)	Ref.
ZIF-67C@rGO[a]/GCE[b]	DPV	0.05	0.5-1000	[27]
Cu-poly(*Cys*)[c]/GCE[b]	LSV	0.37	0.5–400	[28]
AgNPs/IL/CA-SPCE[d]	LSV	0.4	3.1–310; 310–1300	[29]
AgNPs/SF-GR[e]/GCE[b]	DPV	0.05	0.1–20	[30]
Fe_3O_4/N/C@MWCNTs-2-600[f]/GCE[b]	DPV	0.19	1–725	[31]
AP32-4[g]	fluorescence	0.0105	0.025–0.8	[32]
NiMnO@pr-GO[h]/GCE[b]	DPV	0.090	0.1–234	[33]
GO@AgNPs-GCE[b]	Amperometric (i-t)	0.069	0.09–4594	This work

[a] Reduced-Graphene Oxide.
[b] Glassly carbon electrode.
[c] Copper poly(cysteine) film.
[d] Ag nanoparticles/ionic liquid modified screen printed electrode.
[e] Silver nanoparticles/sulfonate functionalized graphene.
[f] Multi-Walled Carbon Nanotubes.
[g] DNA library-immobilized magnetic beads SELEX technology.
[h] Parcel reduced graphene oxide.

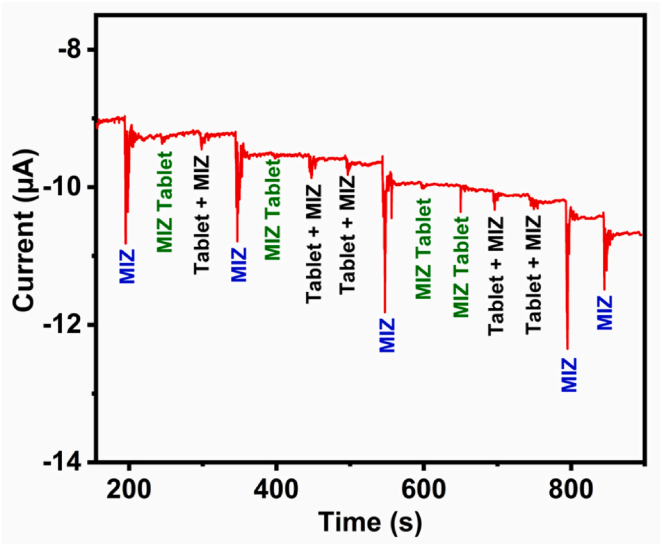

Fig. 7. Amperometric response of real samples studies in 0.05 M PBS (pH 7.2) at applied potential −0.54 V; rpm: 1200.

AgNPs@GO nanocomposites. The prepared composite showed the good intercalation of AgNPS@GO as shown in FESEM. The AgNPs@GO nanocomposites were for electrochemical detection of MIZ. The AgNPs@GO nanocomposites showed a wide-linear range of 0.09 to 4594 μM, LOD value of 69 nM and LQD value of 0.786 μM, respectively. The AgNPs@GO nanocomposites detected the MIZ in pharmaceutical tablets, making it more suitable for applied practice.

Declaration of Competing Interest

The authors declare that they have no known competing financial interests or personal relationships that could have appeared to influence the work reported in this paper.

Acknowledgments

The authors gratefully acknowledge the Department of Botany, Periyar University, Tamil Nadu, India, for selecting as University Research Fellowship (URF) and providing financial assistance, and National Taiwan University of Science and Technology, Taiwan, ROC for this study.

Appendix A. Supplementary data

Supplementary data to this article can be found online at https://doi.org/10.1016/j.sbsr.2021.100425.

References

[1] I. Khan, K. Saeed, I. Khan, Nanoparticles: properties, applications and toxicities, Arab. J. Chem. 12 (2019) 908–931.
[2] J. Jeevanandam, A. Barhoum, Y.S. Chan, A. Dufresne, M.K. Danquah, Review on nanoparticles and nanostructured materials: history, sources, toxicity and regulations, Beilstein J. Nanotechnol. 9 (2018) 1050–1074.
[3] T. Nagamune, Biomolecular engineering for nanobio/bionanotechnology, Nano Convergence 4 (2017) 9.
[4] R. Karthik, R. Sasikumar, Shen-Ming Chen, M. Govindasamy, J. Vinoth Kumar, V. Muthuraj, Green synthesis of platinum nanoparticles using quercus glauca extract and its electrochemical oxidation of hydrazine in water samples, Int. J. Electrochem. Sci. 11 (2016) 8245–8255.
[5] K.S. Siddiqi, A. Husen, R.A. Rao, A review on biosynthesis of silver nanoparticles and their biocidal properties, J. Nanobiotechnol. 16 (2018) 14.
[6] J. Singh, T. Dutta, K.-H. Kim, M. Rawat, P. Samddar, P. Kumar, Green'synthesis of metals and their oxide nanoparticles: applications for environmental remediation, J. Nanobiotechnol. 16 (2018) 84.
[7] I. Hussain, N. Singh, A. Singh, H. Singh, S. Singh, Green synthesis of nanoparticles and its potential application, Biotechnol. Lett. 38 (2016) 545–560.
[8] F. Mujeeb, P. Bajpai, N. Pathak, Phytochemical evaluation, antimicrobial activity, and determination of bioactive components from leaves of *Aegle marmelos*, Biomed. Res. Int. 2014 (2014).
[9] T.D. Thang, D.N. Dai, I.A. Ogunwande, Identification of the volatile compounds in the leaf and stem bark of three Goniothalamus species from Vietnam, J. Essential Oil Bear. Plants 19 (2016) 743–749.
[10] V. Palani, M. Shanmugasundaram, V. Maluventhen, S. Chinnaraj, W. Liu, B. Balasubramanian, M. Arumugam, Phytoconstituents and their potential antimicrobial, antioxidant and mosquito larvicidal activities of Goniothalamus wightii Hook. F. & Thomson, Arab. J. Sci. Eng. 45 (2020) 4541–4555.
[11] R. Karthik, Yu-Shen Hou, Shen-Ming Chen, A. Elangovan, M. Ganesan, P. Muthukrishnan, Eco-friendly synthesis of Ag-NPs using Cerasus serrulata plant extract–its catalytic, electrochemical reduction of 4-NPh and antibacterial activity, J. Ind. Eng. Chem. 37 (2016) 330–339.
[12] F. Ban, S. Majid, N. Huang, H. Lim, Graphene oxide and its electrochemical performance, Int. J. Electrochem. Sci. 7 (2012) 4345–4351.
[13] J. Li, D. Kuang, Y. Feng, F. Zhang, Z. Xu, M. Liu, D. Wang, Green synthesis of silver nanoparticles–graphene oxide nanocomposite and its application in electrochemical sensing oftryptophan, Biosens. Bioelectron. 42 (2013) 198–206.
[14] P. Danvirutai, M. Ekpanyapong, A. Tuantranont, E. Bohez, S. Anutrakulchai, A. Wisitsoraat, C. Srichan, Ultra-sensitive and label-free neutrophil gelatinase-associated lipocalin electrochemical sensor using gold nanoparticles decorated 3D graphene foam towards acute kidney injury detection, Sensor Bio-Sens. Res. 20 (2020) 100380.
[15] M. Sivakumar, S. Yadav, W.S. Hung, J.-Y. Lai, One-pot eco-friendly synthesis of edge-carboxylate graphene via dry ball milling for enhanced removal of acid and basic dyes from single or mixed aqueous solution, J. Clean. Prod. 121498 (2020).
[16] M. Tefera, M. Tessema, S. Admassie, E.I. Iwuoha, T.T. Waryo, P.G.L. Baker, Electrochemical determination of phenothrin in fruit juices at graphene oxide-polypyrrole modified glassy carbon electrode, Sensor Bio-Sens. Res. 21 (2018) 27–34.
[17] M. Roushani, Z. Rahmati, S. Farokhi, S.J. Hoseini, R.H. Fath, The development of an electrochemical nanoaptasensor to sensing chloramphenicol using a nanocomposite consisting of graphene oxide functionalized with (3-Aminopropyl) triethoxysilane and silver nanoparticles, Mater. Sci. Eng. C 108 (2020) 110388.
[18] M. Sivakumar, K. Pandi, S.-M. Chen, S. Yadav, T.-W. Chen, V. Veeramani, Highly sensitive detection of gallic acid in food samples by using robust NiAl2O4 nanocomposite materials, J. Electrochem. Soc. 166 (2019) B29.
[19] M.A. Deshmukh, B.-C. Kang, T.-J. Ha, Non-enzymatic electrochemical glucose sensors based on polyaniline/reduced-graphene-oxide nanocomposites functionalized with silver nanoparticles, J. Mater. Chem. C 8 (2020) 5112–5123.
[20] H. Huang, K. Shan, J. Liu, X. Tao, S. Periyasamy, S. Durairaj, Z. Jiang, J.A. Jacob, Synthesis, optimization and characterization of silver nanoparticles using the catkin extract of Piper longum for bactericidal effect against food-borne pathogens via conventional and mathematical approaches, Bioorg. Chem. 103 (2020) 104230.
[21] C.G. Sørensen, W.K. Karlsson, F.M. Amin, M. Lindelof, Metronidazole-induced encephalopathy: a systematic review, J. Neurol. 267 (2020) 1–13.
[22] M.M. Bottenberg, K.A. Hegge, D.K. Eastman, R. Kumar, Metronidazole -induced encephalopathy: a case report and review of the literature, J. Clin. Pharmacol. 51 (1) (2011) 112–116, https://doi.org/10.1093/cid/ciaa395.
[23] A.E. Vilian, K.S. Ranjith, S.J. Lee, R. Umapathi, S.-K. Hwang, C.W. Oh, Y.S. Huh, Y.-K. Han, Hierarchical dense Ni− Co layered double hydroxide supported carbon nanofibers for the electrochemical determination of metronidazole in biological samples, Electrochim. Acta 354 (2020) 136723.
[24] L.Y. Klimenko, G.L. Shkarlat, Z.V. Shovkova, S.V. Kolisnyk, O.I. Nazarko, New procedures of metronidazole determination by the method of gas-liquid chromatography, Res. J. Pharmacy Technol. 13 (2020) 1157–1166.
[25] Y. Baikeli, X. Mamat, M. Wumaer, M. Muhetaer, H.A. Aisa, G. Hu, Electrochemical determination of metronidazole using a glassy carbon electrode modified with nanoporous bimetallic carbon derived from a ZnCo-based metal-organic framework, J. Electrochem. Soc. 167 (2020) 116513.
[26] S. Ahmed, M. Saifullah, B.L. Ahmad, S. Swami, Ikram, green synthesis of silver nanoparticles using Azadirachta indica aqueous leaf extract, J. Radiat. Res. Appl. Sci. 9 (2016) 1–7.
[27] H. Chen, X. Wu, R. Zhao, Z. Zheng, Q. Yuan, Z. Dong, W. Gan, Preparation of reduced graphite oxide loaded with cobalt (II) and nitrogen co-doped carbon polyhedrons from a metal-organic framework (type ZIF-67), and its application to electrochemical determination of metronidazole, Microchim. Acta 186 (2019) 1–9.
[28] Y. Gu, X. Yan, W. Liu, C. Li, R. Chen, L. Tang, Z. Zhang, M. Yang, Biomimetic sensor based on copper-poly (cysteine) film for the determination of metronidazole, Electrochim. Acta 152 (2015) 108–116.
[29] S. Sadeghi, M. Hemmati, A. Garmroodi, Preparation of ag-nanoparticles/ionic-liquid modified screen-printed electrode and its application in the determination of metronidazole, Electroanalysis 25 (2013) 316–322.
[30] H. Zhai, Z. Liang, Z. Chen, H. Wang, Z. Liu, Z. Su, Q. Zhou, Simultaneous detection of metronidazole and chloramphenicol by differential pulse stripping voltammetry using a silver nanoparticles/sulfonate functionalized graphene modified glassy carbon electrode, Electrochim. Acta 171 (2015) 105–113.
[31] S. Yuan, X. Bo, L. Guo, In-situ insertion of multi-walled carbon nanotubes in the Fe3O4/N/C composite derived from iron-based metal-organic frameworks as a catalyst for effective sensing acetaminophen and metronidazole, Talanta 193 (2019) 100–109.
[32] A. Mao, H. Li, L. Yu, X. Hu, Electrochemical sensor based on multi-walled carbon nanotubes and chitosan-nickel complex for sensitive determination of metronidazole, J. Electroanal. Chem. 799 (2017) 257–262.
[33] A.K. Vivekanandan, V. Subash, S.-m. Chen, S.-H. Chen, Sonochemical synthesis of nickel-manganous oxide nanocrumbs decorated partially reduced graphene oxide for efficient electrochemical reduction of metronidazole, Ultrason. Sonochem. 68 (2020) 105176.